Nanotechnology, Science and Applications

Dovepress
Taylor & Francis Group

Open Access Full Text Article

ORIGINAL RESEARCH

Tailoring CdO-CuO-ZnO Mixed Metal Oxide Nanocomposites for Anticancer Activity via Co-Precipitation Method

Shadha Nasser Aziz[1,2], Abduh Mohammad Abdulwahab[3], Thana Shuga Aldeen[1], Abdullah Ahmed Ali Ahmed[3,4]

[1]Physics Department, Faculty of Science, Sana'a University, Sana'a, Yemen; [2]Department of Basic Sciences, Al-Darb Community College, Dhamar, Yemen; [3]Physics Department, Faculty of Applied Science, Thamar University, Dhamar, 87246, Yemen; [4]Fachbereich Physic and Center for Hybrid Nanostructures (Chyn), Universität Hamburg, Hamburg, 22761, Germany

Correspondence: Shadha Nasser Aziz; Abduh Mohammad Abdulwahab, Email Shd.Aziz@su.edu.ye; abduhabdulwahab@yahoo.com

Introduction: The use of metal oxide nanoparticles as anticancer agents is of great interest due to their unique properties that allow targeted delivery at low concentrations with minimal toxicity to healthy cells.

Methods: In this work, CdO-CuO-ZnO mixed metal oxide nanocomposites were synthesized by the co-precipitation method, and their structural and optical properties, along with their anticancer activity, were investigated. The samples were characterized by X-ray diffraction (XRD), total reflection X-ray fluorescence (TXRF), transmission electron microscopy (TEM), selected area electron diffraction (SAED), UV-Vis spectroscopy, electrometer/high resistance material, and vibrating sample magnetometers (VSM).

Results: X-ray diffraction (XRD) measurements showed that CdO exhibits a cubic structure, CuO possesses a monoclinic structure, ZnO displays a hexagonal structure, and the mixture showed peaks corresponding to all three oxides. TEM images revealed that the prepared nanoparticles have quasi-spherical shapes. Anticancer studies confirmed that the CdO-CuO-ZnO nanocomposite demonstrates excellent cytotoxicity, with moderate activity against human colon (Caco-2) and lung (A549) cancer cell lines, exhibiting IC50 values of 10.57 µg/mL and 6.61 µg/mL, respectively.

Conclusion: Our study shows that the prepared CdO-CuO-ZnO nanocomposite has massive potential in cancer therapy.

Keywords: Co-precipitation, CdO-CuO-ZnO nanocomposite, Anti-cancer activity, Cytotoxic effect

Introduction

Nanoparticles (NPs) have garnered significant attention over the last decade for both commercial and medical applications due to their diverse range of properties. They are used in the production of numerous consumer goods, including clothing, electronics, computers, food coloring, and food.[1,2] Additionally, they are used in advanced technologies, including photocatalysts, sensors, piezoelectric components, fuel cells, and solar cells.[3–6] Remarkable properties of metal oxide semiconductors include their inherent p-n characteristics, broad light absorption, quick dynamic response, and improved sensitivity to changes in humidity. Basically, the ability to tune bandgap energy by combining two unique materials is a significant benefit in the field of nanotechnology. Additionally, the synthesis of nanocomposite materials with adjustable shapes, sizes, and surface characteristics is crucial for a variety of practical applications.[7,8]

Multi-metal oxide (MMO), ie formed by combining two or more metals in an oxide matrix, could result in the production of novel materials with superior chemical and physical characteristics and a high potential for technological advancement.[9] The synthesis of metal oxide nanocomposites has been accomplished using a variety of techniques, including micro-emulsion synthesis, sol-gel technique, co-precipitation method, hydrothermal processing, microwave-assisted synthesis, wet chemical method, solid-state reaction, etc. The co-precipitation method is the most popular among these due to its effectiveness, low growth temperature requirement, simplicity, quickness, and low cost.[10]

Received: 24 January 2025
Accepted: 3 May 2025
Published: 7 May 2025

Currently, a comprehensive cancer treatment system that combines surgery, chemo, radio, and biologically targeted therapy has been developed. All aforementioned treatments, however, have limitations. Even after four years, patients with tumors still have a very low chance of survival. Clinical experience has demonstrated that, aside from a few specific medications, the majority of current therapies are unable to improve the cure rate of cancer patients. Normal tissue cells may also be harmed by radiotherapy. As a result, researchers and clinicians are exploring alternative cancer treatment approaches to enhance the current system. In recent years, nanomaterials have gained significant popularity in antitumor research. Because of their distinct physicochemical properties, nanoparticles stand out as a prominent example among nanomaterials.[11–15]Consider chemotherapy as an example: the majority of current chemotherapeutic drugs are non-specific cytotoxic agents, which can lead to tumor cells developing drug resistance drugs and cause damage to normal tissue cells.

Despite its inherent toxicity, cadmium (Cd) has shown great promise in anticancer applications. Oxidative stress may originate from CdO nanoparticles (NPs) that produce reactive oxygen species (ROS) within cancer cells. Developments in bioremediation methods and material science, such as the synthesis of less hazardous quantum dot structures, are essential for weighing the advantages and disadvantages of cadmium use. CdO nanoparticles (NPs) induce oxidative stress by generating ROS within cancer cells.[16,17] ROS causes damage to cellular components, including DNA, lipids, and proteins, ultimately triggering apoptosis or necrosis.[18,19] Metal oxides exhibit strong anticancer effects of CdO NPs on various cancer cell lines, indicating their potential as a targeted therapeutic agent. Mazhar et al reported the presence of CdO NPs with other metals (such as Ni).[20] Compared to standards such as doxorubicin, CdO-containing nanocomposites often show similar or enhanced efficacy in vitro, particularly at optimized doses, with IC50 values in the extreme range for specific cancer types.[21] Cadmium oxide (CdO) nanoparticles can be utilized safely by both human and animal cells, despite their anticancer effects. The good news is that when used as anticancer agents, CdO NPs are safe for mammalian cells, including human cells. In developed countries, CdO is frequently produced because of its unique properties. Despite acting similarly to other nanoparticles, CdO is more effective and efficient at rupturing cell walls and eliminating cancerous cells.[22]

The cytotoxic properties of nanoparticles (NPs) are significantly influenced by their size and shape, as demonstrated in numerous previous studies.[23–25] Smaller NPs typically have a larger surface area relative to their volume, which can lead to increased interactions with cellular components and potentially higher cytotoxicity. For instance, NPs showed the highest ROS production due to their high dislocation density, indicating that the surface defects effectively generated ROS.[23] ROS damages cellular components, including proteins, DNA, and mitochondria, amplifying cytotoxicity. Moreover, cellular uptake is influenced by the size of NPs, as smaller NPs are more efficiently internalized via endocytosis, enabling deeper penetration into cells and tissues.[23,24] Additionally, the shape of NPs plays a crucial role in determining their cytotoxicity, particularly in terms of membrane interactions, immune evasion, and targeting, as well as intracellular trafficking.[25] Anisotropic shapes, such as polyhedral and rod-like structures with sharp edges or high aspect ratios, induce mechanical stress, causing membrane puncture and leakage of cytoplasmic content, thereby enhancing cytotoxicity.[24] In contrast, spherical NPs exhibit lower cytotoxicity due to their smoother surfaces and reduced physical damage during cellular uptake.[23,25,26] Moreover, the association of size/shape with cytotoxicity, which leads to mechanisms such as oxidative stress, ion release, protein formation, … etc, plays a crucial role in influencing their cytotoxic properties. The oxidative stress generated by the smaller NPs and defect-rich shapes produces more ROS, overwhelming cellular antioxidant defenses.[23,25] The release of metallic ions from metal oxide NPs depends on the size and shape of the NPs. Smaller particles release ions more rapidly, resulting in acidic environments that lead to enhanced ROS generation and increased cytotoxic effects. Size and shape alter protein adsorption patterns, influencing immune recognition and cellular interactions.[24]

The surface, size, and structure characteristics of nanomaterials make them effective anticancer agents. CdO, CuO, and ZnO are metal oxide nanoparticles that are excellent anticancer agents that may be utilized to treat a variety of cancer-related malignant tumors, including lung (A549) cancer, human hepatoblastoma (HepG2), breast carcinoma (MCF-7), and colon cancer (Caco-2).[20,27–30] Jana et al investigated α Fe2O3–ZnO nanocomposite prepared via the core-shell method and its antibacterial and anticancer activities.[31] According to Hanan et al, the ZnO/CdO mixed metal oxide exhibits anticancer activity.[32] The photocatalytic and biological activities of the CdO-MgO nanocomposite

prepared by microwave synthesis have been described by Karthik et al.[33] Elias et al investigated comparative studies in the UV–Vis spectroscopy, photoluminescence, and cytotoxicity of Cu_2O/CuO, ZnO NPs, and Cu_2O/CuO–ZnO NPs.[34] Lefojane et al utilized the green chemistry route to synthesize a CdO/$CdCO_3$ nanocomposite. CdO/$CdCO_3$ nanocomposite has a selective cytotoxic effect on breast cancer cells.[35] The study by Skheel et al focuses on the environmentally friendly production of CdO NP S by employing turmeric plant extract as a covering and reducing agent. Human colon cancer cells (HT29) were shown to be significantly inhibited by green-synthesized CdO_x NPs nanoparticles.[36] Mazhar et al investigated $Cd_{1-x}Ni_xO$ synthesized using the co-precipitate calcination technique. The cytotoxicity effect of the prepared $Cd_{1-x}Ni_xO$ samples was assessed on four cancer cell lines: human hepatoblastoma (HepG2), human lung adenocarcinoma (A549), human breast cancer (MDA-MB231), and breast carcinoma (MCF-7).[20]

Our knowledge indicates that the mixing of metal nanoparticles has been a significant subject matter of recent research. This work focuses on mixing three metal oxides and characterizing the resulting samples using various physical techniques, including analysis of their structural and optical properties. Mixing these metal oxides can enhance their properties. By using the co-precipitation method, we will produce CdO, CuO, ZnO (NPs), and mixed metal oxides of (CdO-CuO-ZnO). Considering that the anticancer effects of the nanocomposite have been under-researched, our research aims to determine how the nanocomposite affects cancer cells.

Experimental Details

Materials

Distilled water (DW), Cadmium nitrate terthydrate ($Cd(NO_3)_2.4H_2O$) (99%) (HIMEDIA), Copper nitrate trihydrate ($Cu(NO_3)_2.3H_2O$) (98%) (HIMEDIA), Zinc nitrate hexahydrate ($Zn(NO_3)_2.6H_2O$) (99%)(HIMEDIA), Sodium hydroxide NaOH (98%) (HIMEDIA) are utilized in this study.

Preparation of CdO, CuO, and ZnO Nanoparticles

($Cd(NO_3)_2{\cdot}4H_2O$) was dissolved in 100 mL of distilled water while being continuously stirred for ten minutes. The solution is obtained by adding 0.1 M NaOH dropwise to the solution to neutralize the acidity and adjust the pH to 7. This adjustment was performed while the solution was continuously stirred for 1 hour at room temperature. The finished solutions are stored for the night in an airtight container. After repeatedly cleaning with distilled water and drying at 100° C for one hour, a mortar and pestle are used to grind the precipitate into a fine powder. To synthesize the nanoparticles, the powder is finally annealed for 2 h at 500 °C. For the other two oxides (CuO and ZnO), these procedures were repeated using $Cu(NO_3)_2{\cdot}3H_2O$ and $Zn(NO_3)_2{\cdot}6H_2O$ as starting materials.

Synthesis of CdO-CuO-ZnO Nanocomposite

The CdO-CuO-ZnO nanocomposite was prepared by dissolving 0.03 M copper nitrate, zinc nitrate, and cobalt nitrate in 300 mL of distilled water, with continuous stirring for 10 minutes. The exact process was utilized for producing CdO, CuO, and ZnO, which were then used for producing the nanocomposite (Figure 1).

Characterization

The structural properties of the prepared CdO, CuO, ZnO (NPs), and CdO–CuO–ZnO nanocomposite were investigated using the XRD technique (XD-2 X-ray diffractometer using CuK_α (λ = 1.54 Å) at 36 kV and 20 mA, China). The concentrations of each element in the samples were measured using a TXRF (xrf,s8 tiger, German), in the Yemeni Geological Survey and Minerals Resources Board. TEM (JEM-2100, Japan) was used to calculate the nanoparticle size. ImageJ software was used to evaluate the size of TEM images. The diffuse reflectance (DR) spectrum of the as-prepared CdO, CuO, ZnO, and CdO-CuO-ZnO nanocomposites was measured using (UV–Vis–NIR) spectrophotometer (Cary 5000-model DRA-2500) over the wavelength range of 400–700 nm (Model: JASCO, (V-750, Japan)). The photoconductivity studies were carried out using the Keithley source meter [Model: Keithley 6517B electrometer/high resistance meter, USA]. The magnetization versus coercivity of the calcined samples was measured using a VSM (Model: Lake 7410, USA) at the Egypt National Research Centre. Cell Lines cancer cells were obtained from the American Type

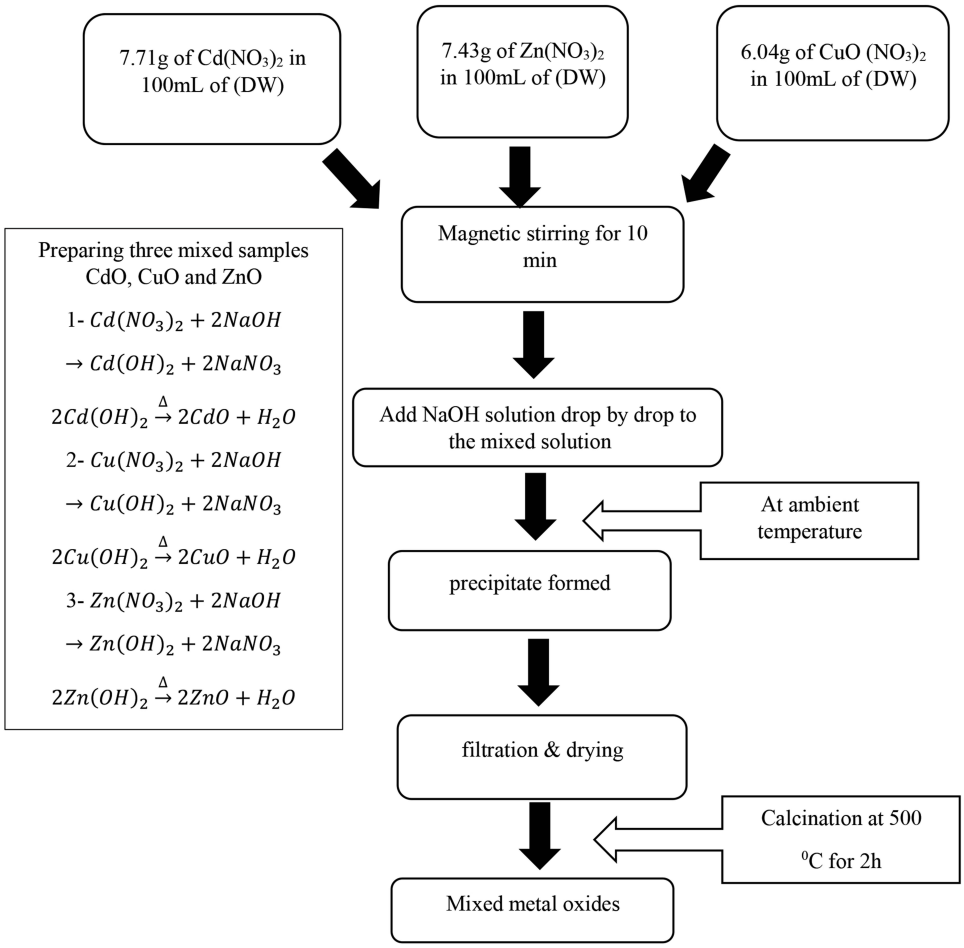

Figure 1 Flowchart of preparation the CdO, CuO, ZnO (NPs) and CdO-CuO-ZnO nanocomposite.

Culture Collection; cells were cultured using DMEM (Gibco, USA) supplemented with 10% FBS (Gibco, USA) and 1% penicillin-streptomycin mixture (100 IU/mL penicillin and 0.1 mg/mL streptomycin). All other chemicals and reagents were from Sigma or Invitrogen.

Anticancer Activity

Cells were seeded at a density of 2–2.5×10^4 cells/well at a 96-well tissue culture plate containing a volume of 180µL complete growth medium per well for 24 hours before being treated with 20 µL different dilutions of the tested compound. Drug stock solutions were prepared in DMSO. Eight concentrations (300, 100, 30, 10, 3, 1, 0.3, and 0.1 µg/mL) were prepared for each compound in the growth media. Cells were then treated for 72 h.

Then, each well received a dose of freshly prepared MTT salt (5 mg/mL; Sigma). The MTT solution was carefully removed, and each well received an equal amount of (200 L) DMSO before being incubated for 60 minutes with shaking. The Multiskan® EX (Thermo Scientific, USA) MicroPlate Reader was utilized to measure the absorbance of each well at 590 nm in order to identify cell proliferation. The experiment was run in triplicate three times. The non-linear fit of the dose-response curve in GraphPad Prism was used to calculate the IC50 values.

Results and Discussion

Structural Analysis

The phase identification and crystal structure were studied utilizing XRD data. The (NPs) XRD pattern confirms the presence of the phases cubic CdO, monoclinic CuO, and hexagonal ZnO. The diffraction peaks match the typical JCPDS Card No. well. CdO (01–1049), CuO (048–1548), and ZnO (01–1136), likewise, CdO-CuO-ZnO nanocomposite (Figure 2).

The diffraction peaks of CdO, CuO, and ZnO can be observed in the multi-metal oxide composite pattern, as shown in Figure 2. Due to the close diffraction angles, some of the diffraction peaks of metal oxides in the XRD pattern of the composite were shifted. The peaks of CdO in the CdO-CuO-ZnO nanocomposites have the highest intensities, and CuO has the lowest in the mixture.

The average crystallite sizes of each phase were calculated using full width at half maximum calculations and whole powder pattern fitting with Scherrer's equation[37–41] (Eq. 1).

$$D = (0.9\ \lambda)/(\beta\ cos\theta) \tag{1}$$

Where λ is the wavelength of the X-ray used, β is the full width at half-maximum intensity (FWHM) (in radians), and θ is the diffraction angle.

To determine the cubic CdO lattice parameters[42,43] (Eq.2):

$$\frac{1}{d^2} = \left[\frac{h^2 + k^2 + l^2}{a^2}\right] \tag{2}$$

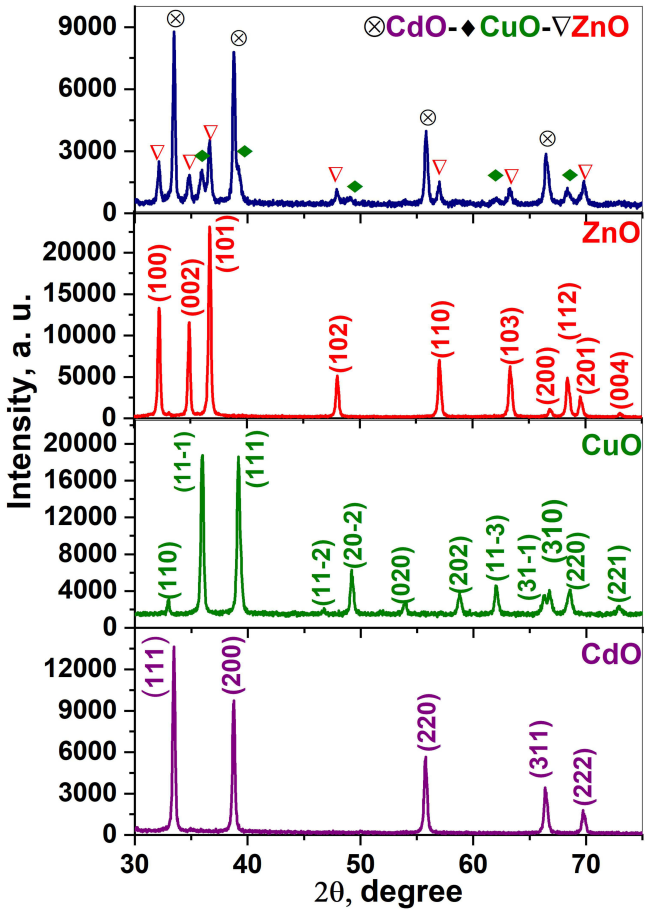

Figure 2 XRD patterns of the CdO, CuO, ZnO (NPs) and CdO-CuO-ZnO nanocomposite.

https://doi.org/10.2147/NSA.S519229

Table 1 XRD Analysis and Particles Size Were Utilized to Determine the Physical Characteristics of the CdO, CuO, ZnO NPs, and CdO-CuO-ZnO Nanocomposite

Sample		a (Å)	b (Å)	c (Å)	Crystallite Size, D_{XRD} (nm)	Particle Size, D_{TEM} (nm)
Single (NPs)	CdO	4.6	–	–	37.73	61
	CuO	4.6	3.4	5.1	30.76	71
	ZnO	3.2	–	5.1	31.79	52
Nanocomposites	CdO	4.6	–	–	36.8	41.5
	CuO	4.7	3.4	5.1	17.2	
	ZnO	3.2	–	5.2	27.2	

For the monoclinic CuO structure, the unit cell parameters a, b, and c were calculated using the relation shown below[42,44] (Eq.3):

$$\frac{1}{d^2} = \frac{1}{sin^2\beta}\left[\frac{h^2}{a^2} + \frac{k^2 sin^2\beta}{b^2} + \frac{l^2}{c^2} - \frac{2hlcos\beta}{ac}\right] \tag{3}$$

To determine the hexagonal ZnO structure, the unit parameter a and c lattice parameters (Eq.4):[45]

$$\frac{1}{d^2} = \frac{4}{3}\left[\frac{h^2 + hk + k^2}{a^2}\right] + \frac{l^2}{c^2} \tag{4}$$

There is a slight increase in the lattice parameters of CuO and ZnO resulting from the nanocomposite mix, as shown in Table 1.

It is clear that mixing the studied nanocomposites raised the dislocation density while lowering the crystallite size. The reduction in crystallite size often corresponds to a greater density of dislocations and defects in the crystal lattice. By upsetting the regular atomic arrangement, these defects result in microstrain. Reducing the crystal size improves the efficiency of both photolysis and biological processes. This outcome was in line with Munawar et al[46] findings regarding the impact of grain size on the overall stress of the nanocomposite.

Elemental Analysis

TXRF spectra (Table 2) and histograms Figure 3 show the results of the elemental chemical analysis of prepared samples carried out by TXRF for CdO-CuO-ZnO nanocomposite. CdO, CuO, and ZnO make up the majority of the nanocomposite material. All other elements, including P, S, Ca, Fe, etc, are present in trace amounts. This outcome is consistent with previous studies.[47,48]

Table 2 TXRF Analysis of CdO-CuO-ZnO Nanocomposite

Compound	Wt%	Elemental	Wt%
CdO	42.69%	Cd	34.85%
CuO	17.83%	Cu	14.41%
ZnO	39.10%	Zn	30.98%
–	–	O	19.38%

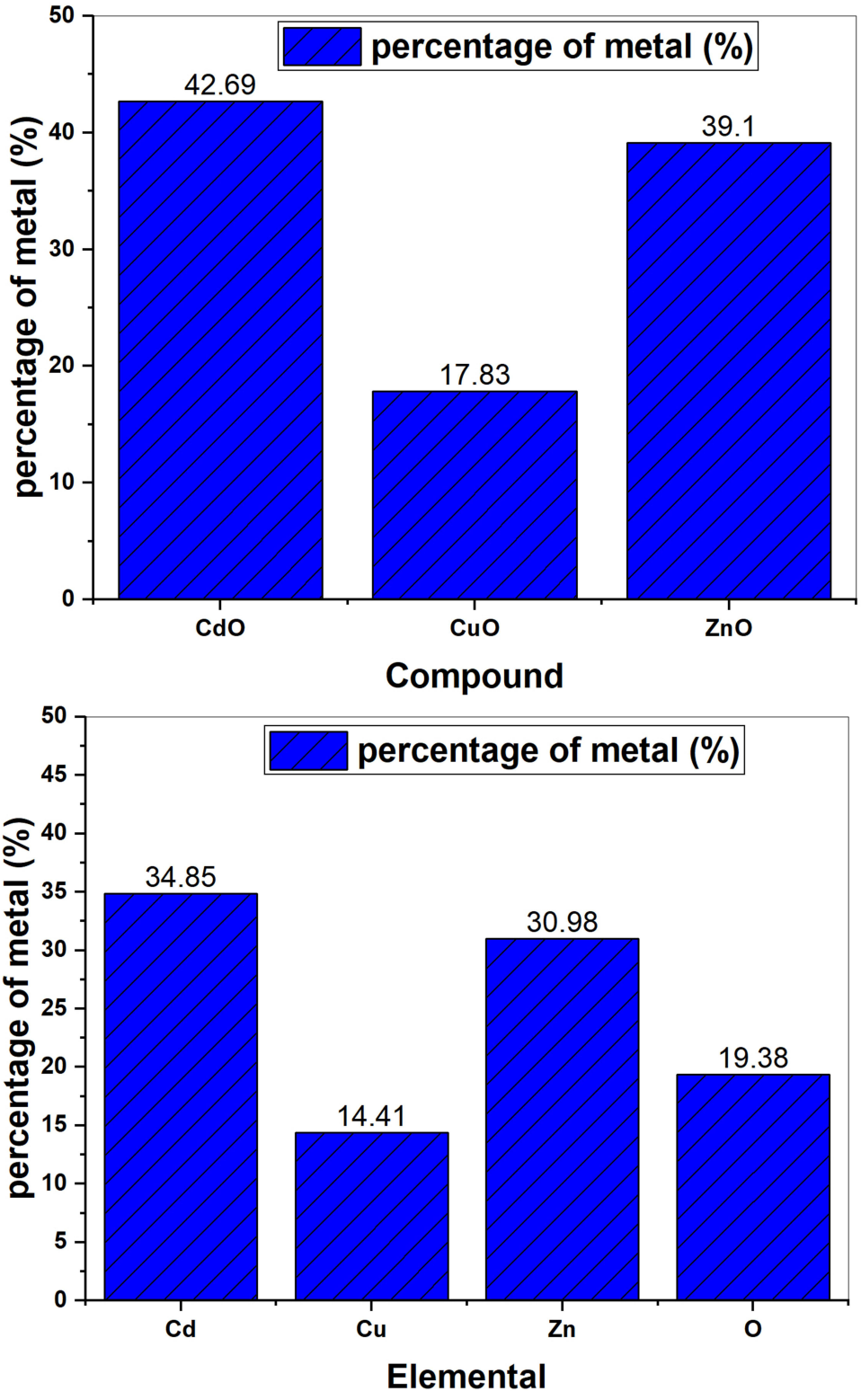

Figure 3 TXRF of CdO-CuO-ZnO nanocomposite.

https://doi.org/10.2147/NSA.S519229

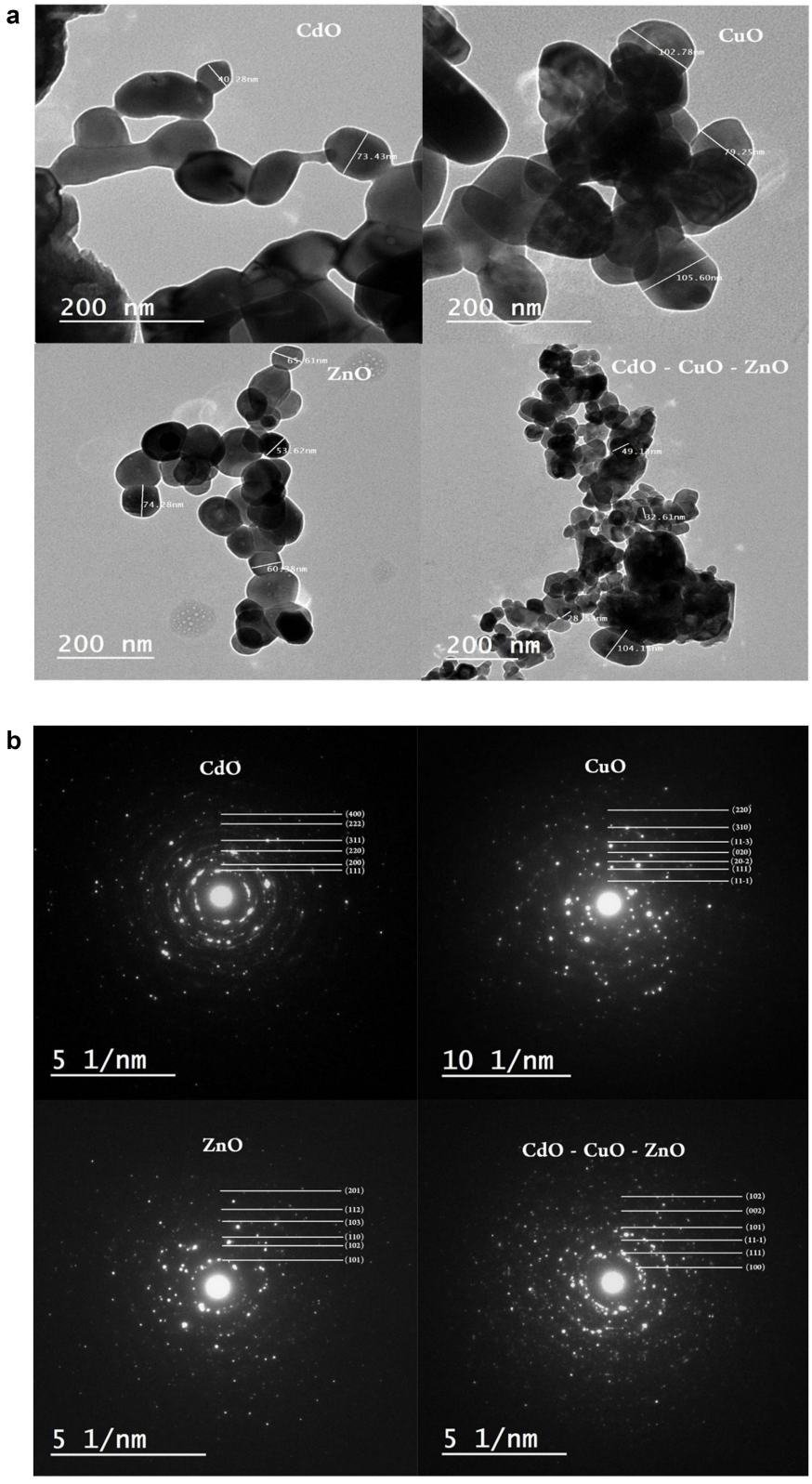

Figure 4 Continued.

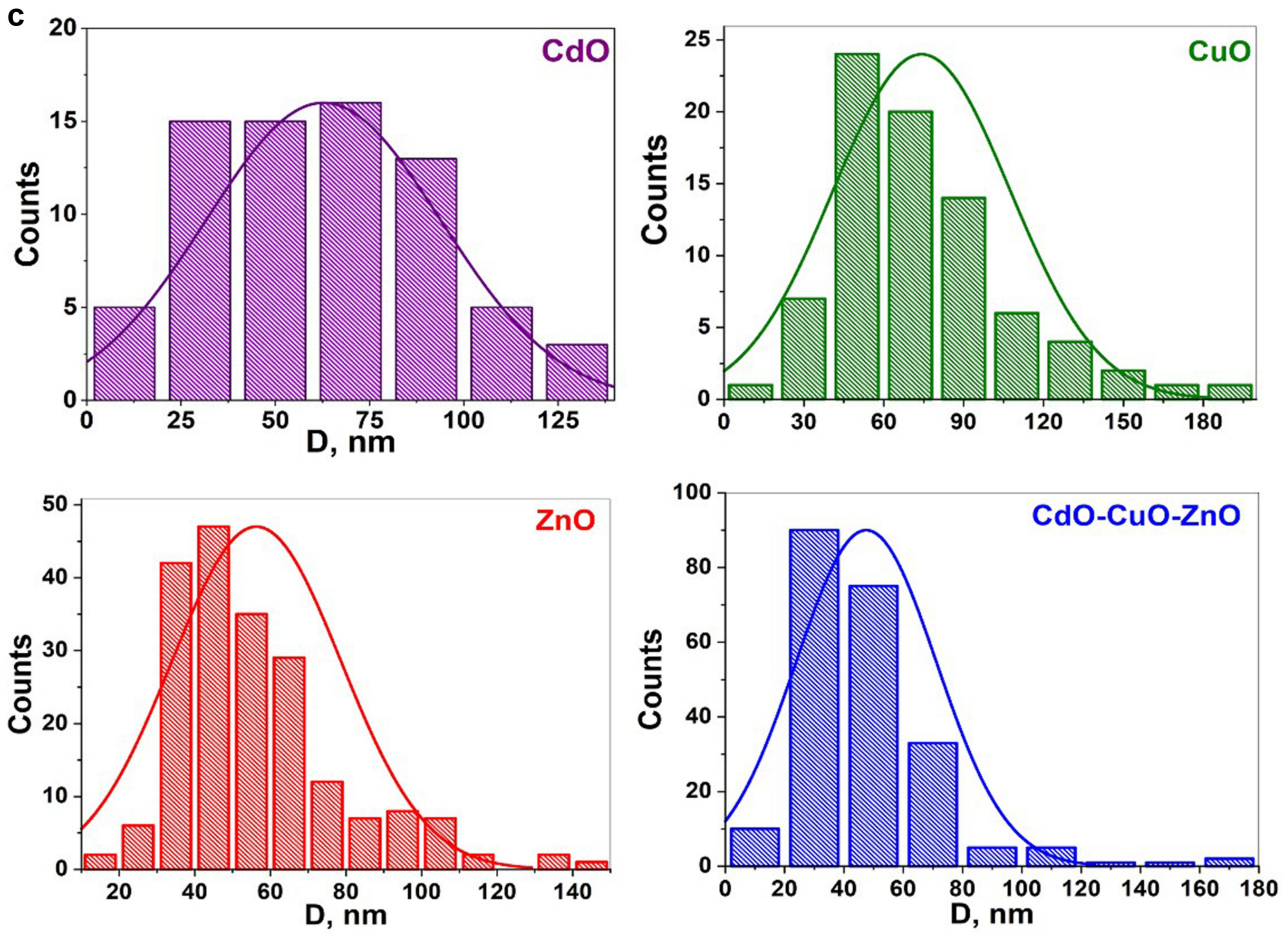

Figure 4 (**a**) TEM image of the CdO, CuO, ZnO (NPs) and CdO-CuO-ZnO nanocomposite. (**b**) SAED patterns the CdO, CuO, ZnO (NPs) and CdO-CuO-ZnO nanocomposite. (**c**) Histograms calculated from TEM images the CdO, CuO, ZnO (NPs) and CdO-CuO-ZnO nanocomposite.

TEM Analysis

CdO, CuO, ZnO (NPs), and CdO-CuO-ZnO nanocomposite are shown in the TEM images and SAED patterns, displayed in Figure 4a and b respectively. For pure CdO, spherical particles with an average size of 61*nm* can be seen. For pure CuO, spherical particles with an average size of 71*nm* have been observed. For pure ZnO, clumped spherical particles (of about 52*nm*) are seen. The composite shows a mixture of spherical particles. The composite's average particle size was determined to be 41.5 nm. All of the samples had nanosized particles, according to TEM images. The ImageJ program was used to measure particle sizes, and a histogram is presented in Figure 4c. The presence of well-defined concentric rings in the SAED patterns confirms the nanocrystalline nature of all samples. The circular edges in the SAED patterns correspond to the XRD d-spacing of CdO, CuO, ZnO (NPs) and CdO- CuO-ZnO nanocomposite.

Optical Studies

Utilizing diffuse reflectance spectroscopy, the optical properties of synthetic CdO, CuO, ZnO (NPs), and CdO-CuO-ZnO nanocomposite materials were assessed. Figure 5 shows the sample reflectance spectrum as a function of wavelength in the 400–700 *nm* spectral range (a). According to the results, the reflectance spectrum increased for CdO NPs and the CdO-CuO-ZnO nanocomposite. In contrast, for CuO NPs, the reflectance decreased with increasing wavelength. For ZnO NPs, the reflection initially increased to a low value, then decreased with increasing wavelength. The Kubelka-Munk equation was applied to convert the measured reflectance into absorbance.[49,50]

https://doi.org/10.2147/NSA.S519229

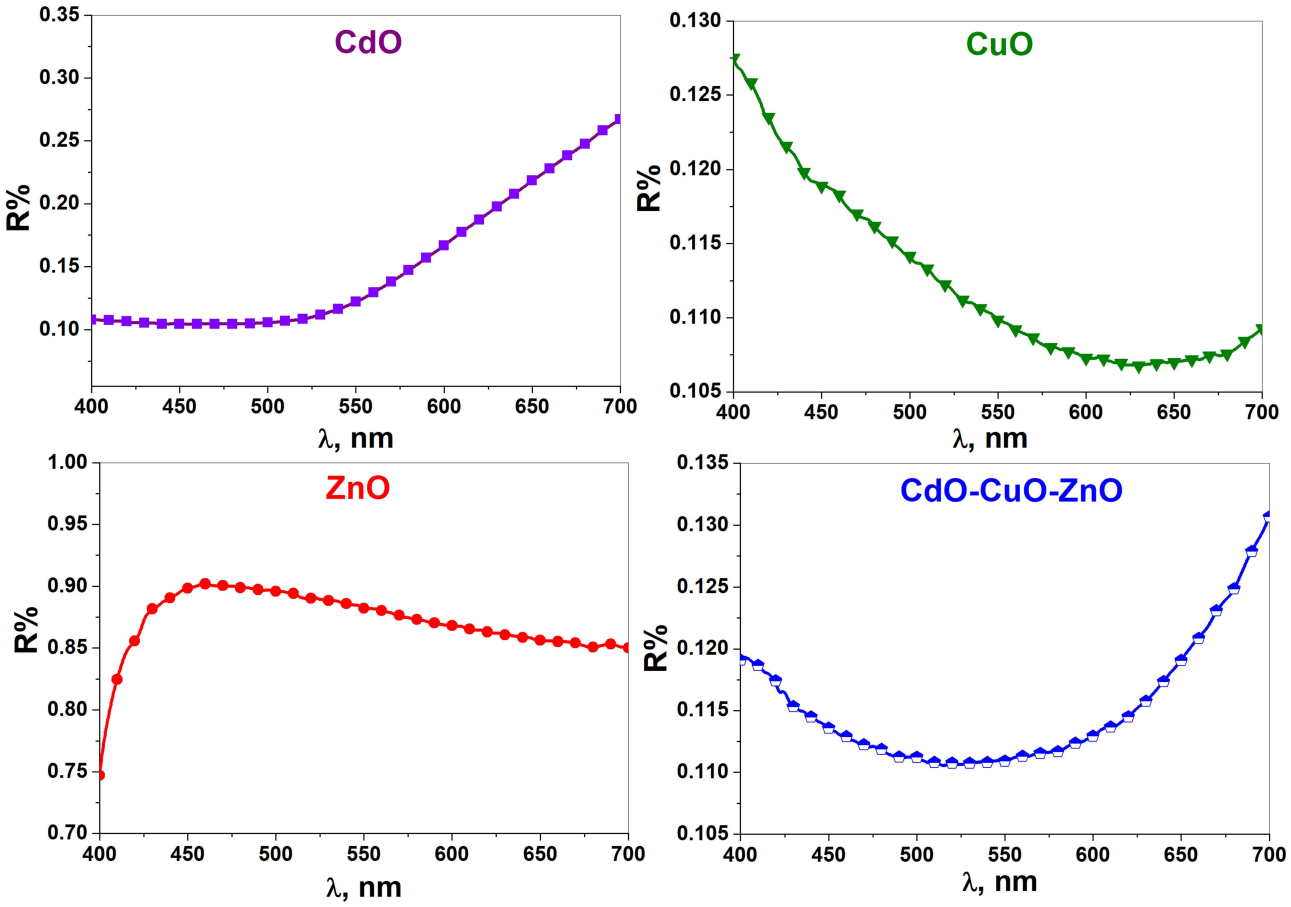

Figure 5 Diffuse reflectance spectrum (R%) of the CdO, CuO, ZnO (NPs) and CdO-CuO-ZnO nanocomposites.

$$F(R) = \frac{(1-R)^2}{2R} \tag{5}$$

Where R is the diffuse reflectance (%) and F(R) is the Kubelka-Munk function corresponding to the absorbance (Figure 5). Utilizing the modified K-M equation, the material's bandgap energy (E_g) and the type of optical transition between the valence band (VB) and conduction band (CB) were identified:[51,52]

$$(F(R)h\upsilon) = A\left(E - E_g\right)^n \tag{6}$$

The type of optical transition is related to the exponent factor n, and the band tailing and material disorder are measured by the constant A, which is dependent on the probability of the optical transition. The energy of the photon is ($E = h\upsilon$). The values of a direct allowed band gap, an indirect allowed band gap, a direct forbidden band gap 1/2, and an indirect forbidden band gap are 2 and 3, respectively. To calculate the material's E_g, plot $(F(R)h\upsilon)^{(1/n)}$ versus E and extrapolate the linear portion of the plot up to $(F(R)h\upsilon)^{(1/n)} = 0$.[51,53]

The type of transition is determined by the best linear fit utilizing various values of n, and this kind of representation is referred to as a Tauc model. The Tauc plot for the CdO-CuO-ZnO nanocomposite $(F(R)h\upsilon)^2 vsE$ and the as-prepared CdO, CuO, and ZnO (NPs) are shown in Figure 6. We obtained the $E_g$values shown in Table 3.

In comparison to the bandgap energies of CdO, CuO, and ZnO (NPs), the extrapolated bandgap value of the CdO-CuO-ZnO nanocomposite is close to that of CuO. Decreasing crystalline size and particle size can both lead to a decrease in the energy gap of synthesis materials through mechanisms such as the influence of surface states. These effects are

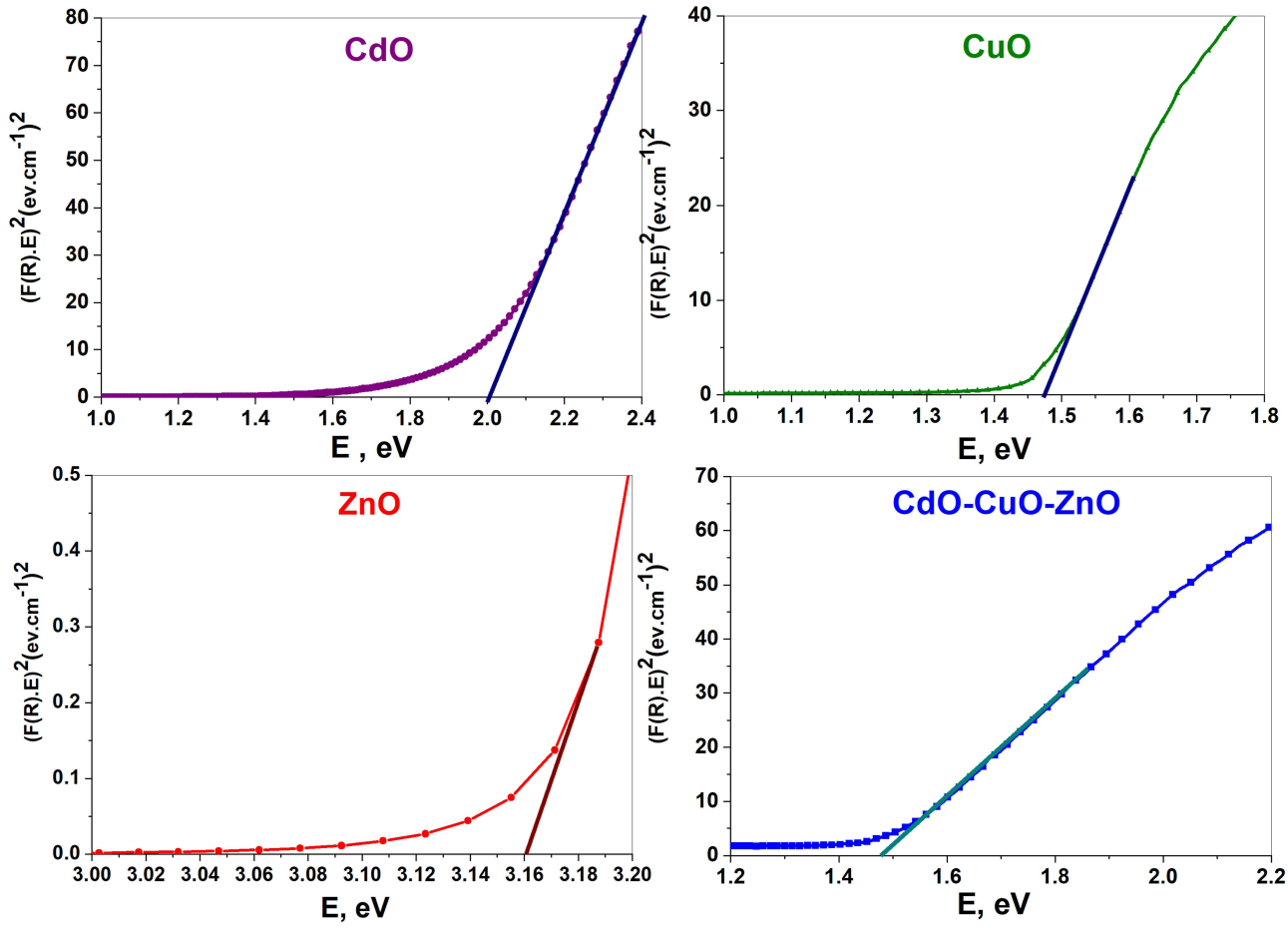

Figure 6 The plot of $(F(R)h\nu)^2$ vs E (eV) for direct band gap.

fundamental to understanding and engineering the electronic properties of nanomaterials and have important implications for various applications in electronics, photonics, and optoelectronics.[54] The UV-Vis results suggest that the combination of three semiconductors may affect the band structure, bactericidal effects, and light-absorbing capacities of the CdO-CuO-ZnO nanocomposite photocatalyst. This result is consistent with Muhammad Ishfaq et al.[55]

Table 3 Optical Bandgap Energy Calculators for the Prepared Sample

Sample	$E_g(eV)$
CdO	2
CuO	1.47
ZnO	3.16
CdO-CuO-ZnO	1.5

https://doi.org/10.2147/NSA.S519229

Table 4 Zeta Potential and Particle Size for the CdO, CuO, ZnO (NPs), and CdO-CuO-ZnO Nanocomposite

Samples	Zeta Potential (*mV*)	Size Distribution (*nm*)
CdO	−20.5	3242
CuO	−22.8	933
ZnO	4.40	634
CdO-CuO-ZnO	5.77	841.3

Zeta Potential and Size Distribution

Determining the zeta potential is an essential method for estimating the surface charge of nanoparticles; it aids in assessing the colloidal stability of NPs. The size of nanoparticles in a colloidal solution is a crucial consideration for their application

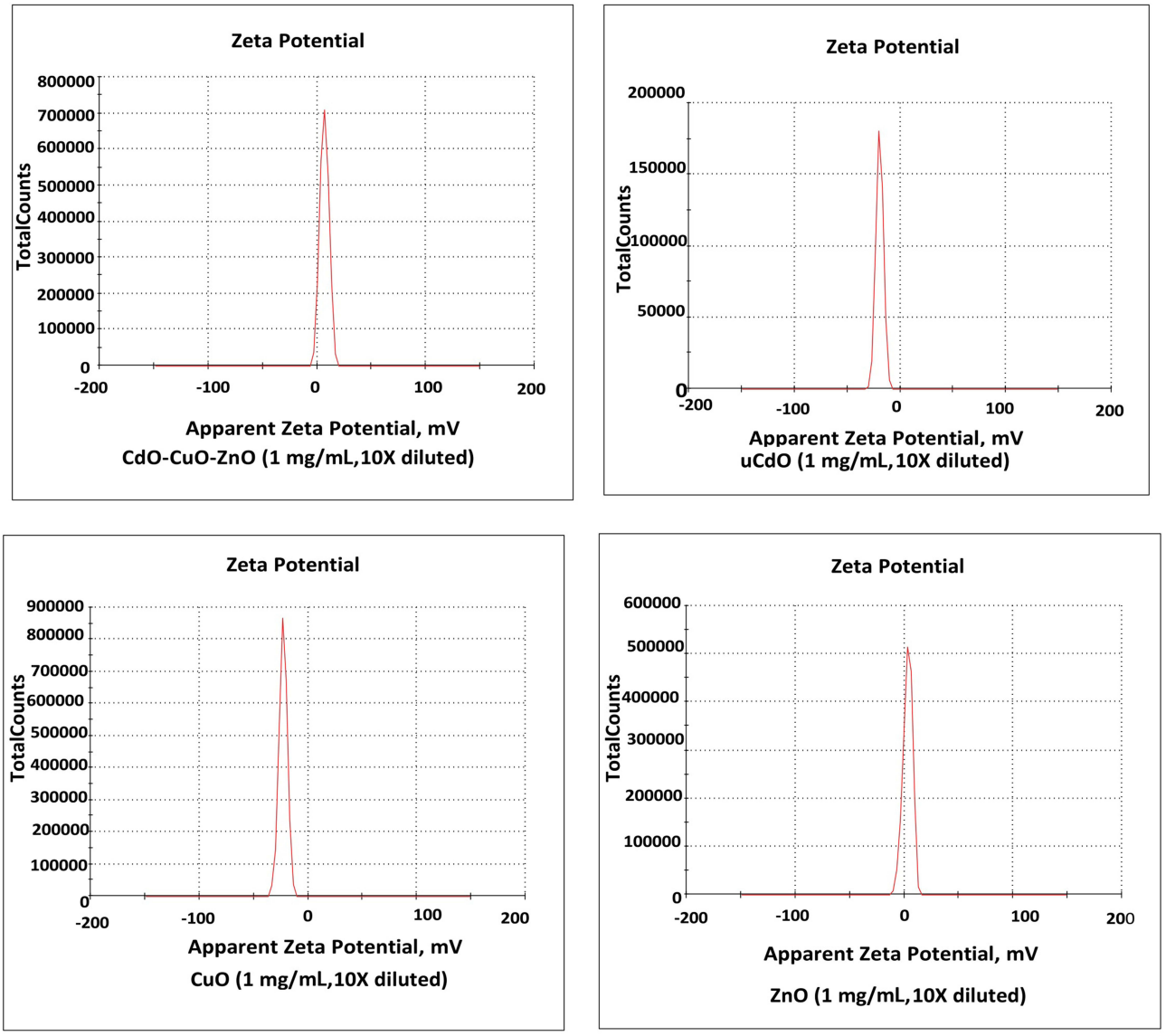

Figure 7 Zeta Potential Distribution the CdO, CuO, ZnO (NPs), and CdO-CuO-ZnO nanocomposite.

in various domains, particularly those in biomedical fields. One well-liked and effective technique for figuring out the size of particles in a colloidal solution is dynamic light scattering or DLS.[56,57] The Zeta potential values between −30 mV and +30 mV indicate poor colloidal stability and are likely to experience flocculation and agglomeration.[58]

The zeta potential and size distribution were used to analyze the stability behavior of synthesized CdO, CuO, ZnO (NPs), and CdO-CuO-ZnO nanocomposite, as shown in Table 4 and Figure 7. The mean size distribution of the CdO, CuO, ZnO (NPs), and the CdO-CuO-ZnO nanocomposite ranged from 634 to 3242 nm in diameter. Consistent with our analysis, the average particle size reported by DLS was larger than the one determined by TEM. The discrepancy between TEM and DLS is consistent with many other studies that reported synthesizing a variety of NPs.[58]

Due to the swelling of CdO, CuO, and ZnO nanoparticles, as well as the CdO-CuO-ZnO nanocomposite in an aqueous medium, the sizes of the nanoparticles, as determined by DLS and TEM, differ. For the CdO, CuO, ZnO (NPs), and CdO-CuO-ZnO nanocomposite, the corresponding zeta potentials were –20.5, –21.7, 2.78, 12, and 5.77 mV. However, ZnO NPs and the CdO-CuO-ZnO nanocomposite were less stable than CdO and CuO NPs. This outcome aligns with the findings of Hussein.[59]

Anticancer Activity

Mitochondria are the primary intracellular ROS source. Nearly all organelle species are known to be oxidized by the most reactive ROS, called OH radicals. ROS produced in the cell generates O^{2-} via electron capture on the surfaces of the nanocomposite and nanoparticles. Free radicals contribute to an imbalance in the oxidant/antioxidant phenomena of the cell by oxidizing lipids, denaturing proteins and nucleic acids, and activating an antioxidant defense system.[60,61]

In lysosomes, reactive oxygen species (ROS) can damage cellular redox disequilibria, lead to DNA point mutations, and impair mitochondrial respiration and apoptosis. ROS can also peroxide the lipids in cell membranes. H_2O_2 is produced in the cytoplasm, where it undergoes the Fenton reaction to generate OH, which damages DNA, causes cellular death, and readily diffuses across mitochondrial membranes. High intracellular ROS levels support the expression of redox-sensitive signaling pathways and death receptor nanoparticles under conditions of typical oxidative stress.[62,63] The toxicity of the nanocomposite to cells is shown in Figure 8.

The information is displayed as the average of the IC50 values from three distinct experiments. Drug stock solutions were prepared in DMSO. Eight concentrations (300, 100, 30, 10, 3, 1, 0.3, and 0.1 µg/mL) were tested, with MTT at a

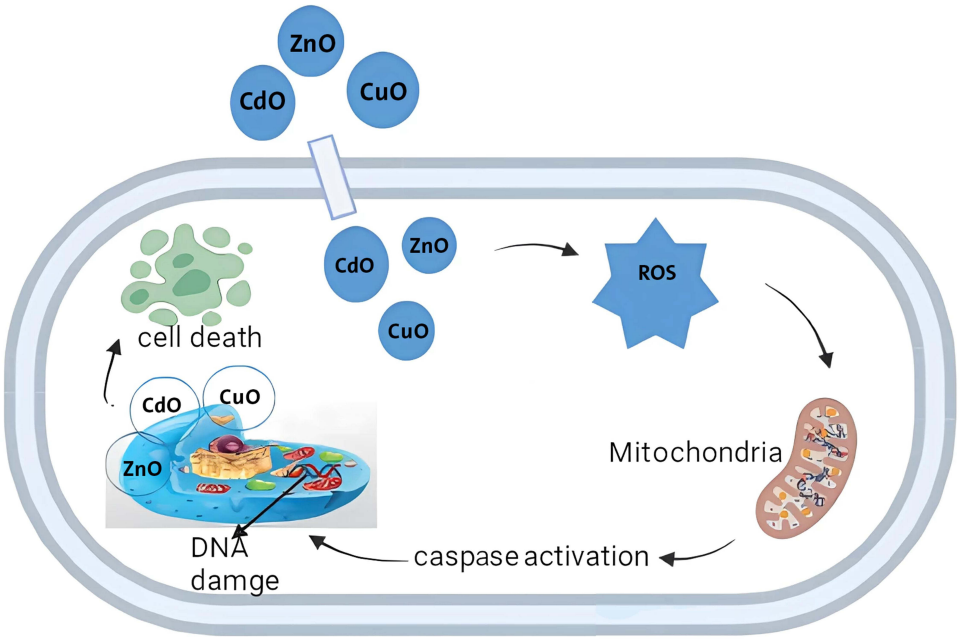

Figure 8 The mechanism underlying the cytotoxicity activity of CdO-CuO-ZnO nanocomposite is depicted schematically.

https://doi.org/10.2147/NSA.S519229

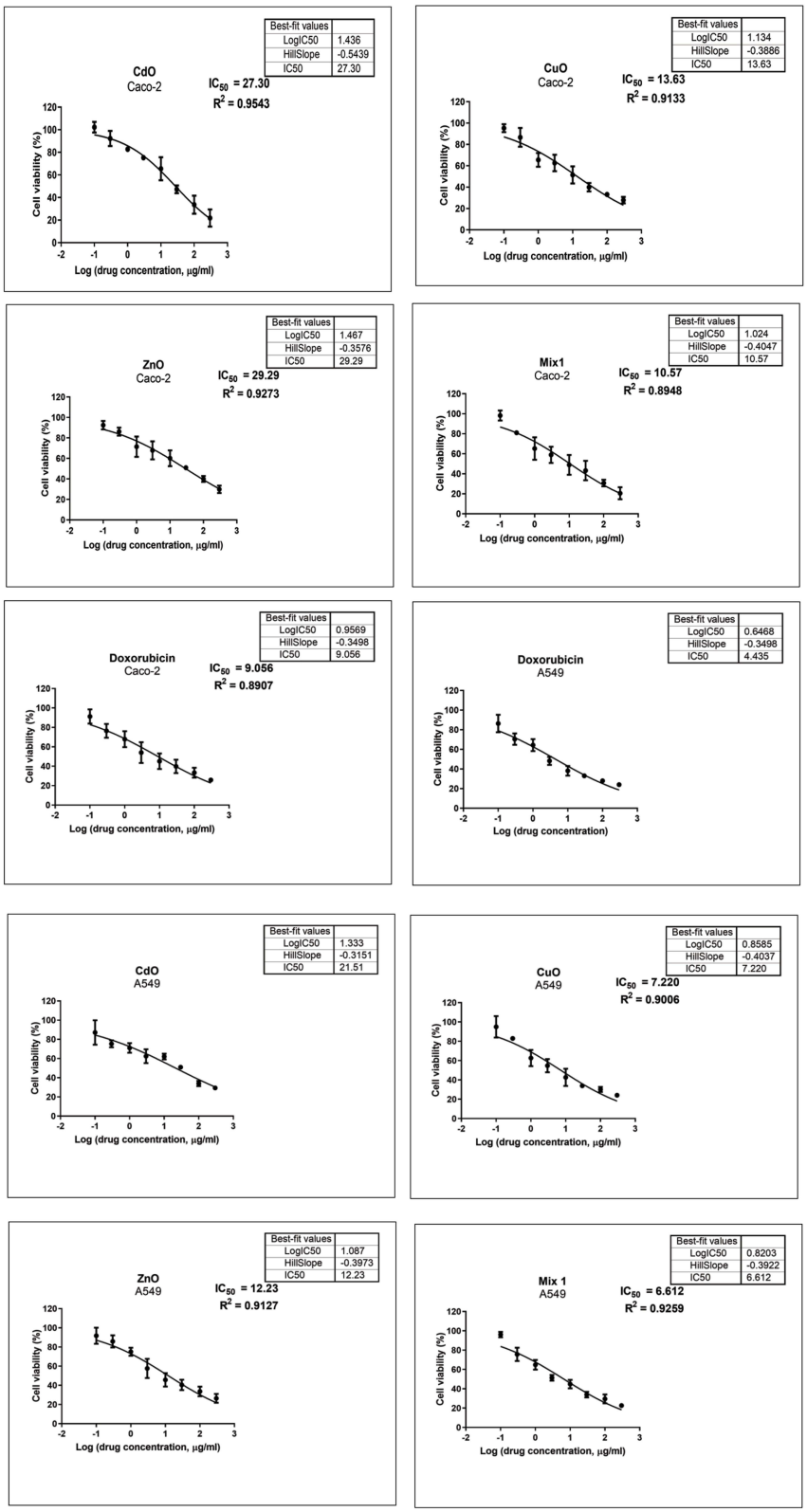

Figure 9 Cell viability% versus logarithm of Concentration IC50 values obtained for samples.

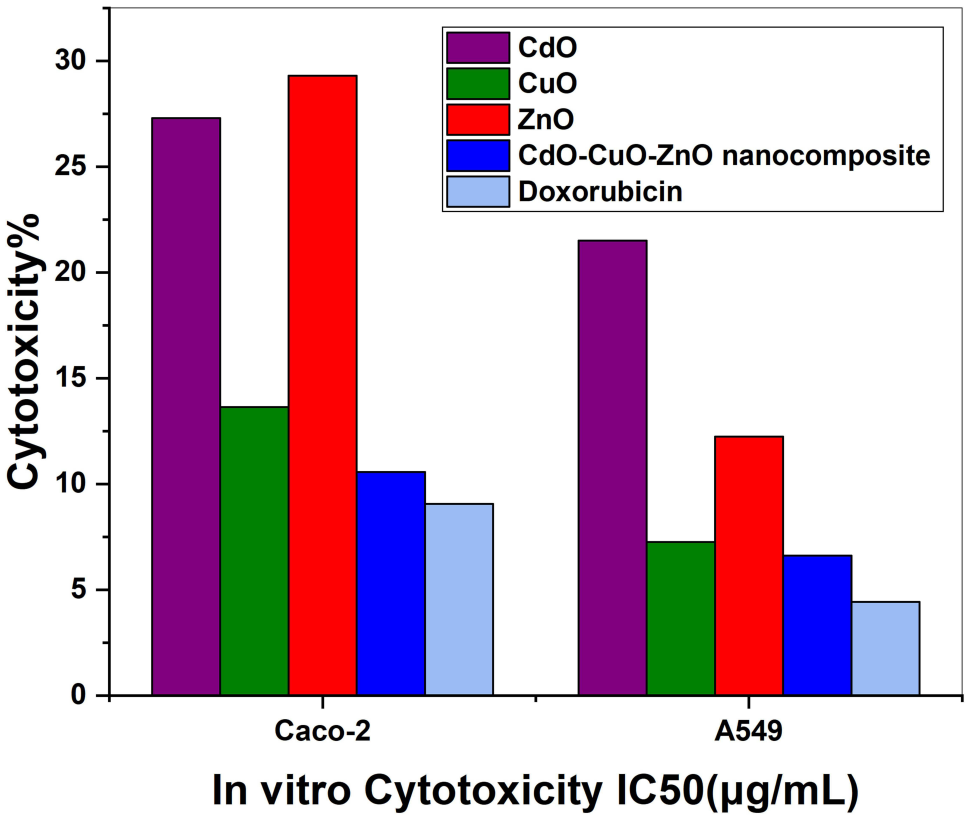

Figure 10 Percentage cytotoxicity of Caco-2 and A549 cells after incubation with CdO, CuO, and ZnO (NPs), and CdO-CuO-ZnO nanocomposite.

final concentration of 0.5 mg/mL, using the Multiskan® EX Microplate Reader (Thermo Scientific, USA) to measure each well's absorbance at 590 nm. Utilizing GraphPad Prism 8's dose-response curves, the experiment was run three times in triplicate to determine the IC50 values. The cell viability data (obtained by the MTT experiment) was plotted against the logarithm of the concentration and IC50 values for the prepared samples and doxorubicin Figure 9. Where IC50 (mg):1–10 (Very strong), 11–20, (strong), 21–50 (moderate), 51–100 (weak) and above 100 (non-cytotoxic).[21]

According to the previous reference,[21] CuO (NP) has been shown to be strong for cancer, while CdO NPs are moderate. ZnO NPs are strong for A549 and moderate for Caco-2. The CdO-CuO-ZnO nanocomposite is effective against both types of cancer. The mixed oxides are better as anti-cancer substances compared to the single oxides, as shown in Figure 10 and Table 5.

Although metal oxide nanocomposites exhibit varying toxicity profiles depending on their physicochemical properties (size, surface area, shape, aspect ratio, and surface functionalization), cell types, cytotoxicity mechanisms, and exposure conditions, these nanocomposites exhibit an influence on cell viability by causing the death of cancer cells while having a negligible effect on normal cells. Sabour et al demonstrated that the Ag and Se dual-doped ZnO-CaO-CuO nanocomposite exhibits stronger toxicity against cancerous Huh-7 cells compared to normal L929 cells. These nanocomposites can inhibit cancer lines in a dose-dependent procedure, while there is no inhibitory influence against normal cells.[64] In another study, the mixed FeO-MnO nanostructure showed significant anticancer activity against lung cancer cells while having low cytotoxicity against normal cells.[65] Elsayed et al have investigated the anticancer efficacy of ZnO-Ag nanocomposites against the cancer cell lines (HCT-116 and HELA) without having an impact on the normal cells.[66] In these studies, as well as numerous published literature reports, metal oxide nanocomposites have been explored for their high anticancer activity against cancerous cells, with minimal effect on normal cells. This characteristic distinguishes them as having a selective affinity for cancerous cells, making them promising anticancer materials.

Table 5 In vitro Anti-Proliferative Activities of the Tested Compounds Against Human Colon (Caco-2) and Lung (A549) Cancer Cell Lines Treated for 72 h

Comp.	Code	In vitro Cytotoxicity IC50 (μg/mL)[a]	
		Caco-2	A549
1	CdO	27.30	21.51
2	CuO	13.63	7.25
3	ZnO	29.29	12.23
4	CdO-CuO-ZnO	10.57	6.61
Doxorubicin		9.05	4.43

Through oxidative stress mechanisms, the cytotoxic effects of metal oxide nanoparticles on cancer cell lines are strongly influenced by their optical bandgap energy. Reactive oxygen species (ROS) are produced more easily when the bandgap is smaller, which increases oxidative stress and the cytotoxicity of cancer cells. For example, a study on zinc oxide (ZnO) nanoparticles showed that lowering the band gap energy increased the production of ROS, which in turn caused oxidative stress and autophagy-mediated apoptosis in cancer cells.[67] Similarly, studies on aluminum-doped ZnO nanoparticles have demonstrated that, in human breast cancer cells (MCF-7), doping increases the bandgap energy of the nanoparticles and enhances their cytotoxicity and oxidative stress response. According to the study, ZnO nanoparticles' band gap energy increased with Al-doping from 3.51 eV for pure ZnO to 3.87 eV for Al-doped ZnO, improving their selective cytotoxicity toward MCF-7 cells while having no effect on normal cells.[68] In their investigation of silver-doped titanium dioxide (Ag-TiO_2) nanoparticles, Ahamed et al discovered that doping with silver decreased the band gap energy, which in turn increased the generation of reactive oxygen species (ROS); human lung (A549) and breast (MCF-7) cancer cells experienced increased oxidative stress and cytotoxicity as a result of this rise in ROS.[69] According to research conducted by Abbas et al, Sn-doped

Table 6 Comparison of Cytotoxicity IC50 Values for Some NPs and Nanocomposites That Have Been Published

Sample	Cell line	Method Used	In vitro Cytotoxicity IC50	References
CdO-Ni	A549	Viability assay	93.349 μg/mL	[20]
CuO	A549	MTT	147.48 μg/mL	[71]
CuO	MCF-7	MTT assay	28.49±3.4 μg/mL	[72]
CuO	CaCo-2	(NRU) assay	12.06 μg/mL	[27]
CuO	CaCo-2	MTT assay	10.04 μg/mL	[27]
ZnO	CaCo-2	PDT	20 ug/mL	[73]
ZnO	Caco-2	MTT assay	36.675 ± 0.916μg/mL	[74]
ZnO	A549	MTT assay	20.45 μg/mL	[75]
$CdO/CdCO_3$	MCF-7	MTT assay	0.65 μg/mL	[35]
Ag/ZnO	A549	MTT assay	19.95 μg/mL	[76]
CeO2@CuO NCs	MDA-MB-231	DPPH assay	10 μg/mL	[77]
Fe2O3@CuO@ZnONPs	Hep-G2 cells	MTT assay	196.4 μg/mL	[78]
CuS	A549	MTT assay	19.10 μg/mL	[79]

CeO_2 nanostructures greatly adjusted the band gap energies, laying the groundwork for massive cellular ROS production that contributes to the death of cancer cells (Neuroblastoma cell lines).[70]

According to these results, the cytotoxic effects of metal oxide nanoparticles on cancer cells may be influenced by adjusting their bandgap energy, which also affects the particles' ability to induce oxidative stress. When synthesizing nanoparticles for targeted cancer treatments, this characteristic can be strategically used. The present cytotoxicity of IC50 is compared with that of some NPs (Table 6).

Conclusions

A novel CdO-CuO-ZnO nanocomposite was synthesized via the co-precipitation method. XRD analysis verified the unique combination of cubic CdO, monoclinic CuO, and hexagonal ZnO structures. Efficient integration of these metal oxides was demonstrated by the nanocomposite's well-defined crystalline structure, in which CdO contributed the highest intensity peaks and CuO the lowest. The composite's nanoscale dimensions were validated by Transmission Electron Microscopy (TEM) analysis, indicating that it has potential for use in biomedical applications. With a measured optical bandgap of 1.5 eV, the nanocomposite shows promise for use in photothermal and photodynamic therapies. Furthermore, the results of the zeta potential analysis revealed that the colloidal behavior of ZnO and CdO-CuO-ZnO nanocomposite was less stable than that of CdO and CuO nanoparticles. The CdO-CuO-ZnO nanocomposite's strong anticancer activity against A549 and Caco-2 cells was one of the study's key findings. The results of the MTT assay showed a significant cytotoxic effect, with IC50 values of 6.61 (μg/mL) for A549 cells and 10.57 (μg/mL) for Caco-2 cells, highlighting the nanocomposite's greater effectiveness compared to individual metal oxide nanoparticles. The observed rise in intracellular ROS levels suggests that apoptosis is a crucial mechanism of action that may be used to target cancer treatments. Overall, this study highlights the superiority of this novel CdO-CuO-ZnO nanocomposite in terms of cytotoxicity and biocompatibility, positioning it as a promising candidate for advanced nanomedicine applications in cancer therapy, particularly with targeted delivery approaches.

Data Sharing Statement

Data will be made available on request.

Acknowledgments

The authors are grateful to the Guinness University of Science and Technology and Thamar University, Dhamar City, Yemen, for their support in facilitating sample processing.

Disclosure

The authors report no conflicts of interest in this work.

References

1. Chibber S, Ansari SA, Satar R. New vision to CuO, ZnO, and TiO 2 nanoparticles: their outcome and effects. *J Nanopart Res*. 2013;15:1–13. doi:10.1007/s11051-013-1492-x
2. Jones CF, Grainger DW. In vitro assessments of nanomaterial toxicity. *Adv Drug Deliv Rev*. 2009;61(6):438–456. doi:10.1016/j.addr.2009.03.005
3. Saravanan R, Karthikeyan S, Gupta VK, Sekaran G, Narayanan V, Stephen A. Enhanced photocatalytic activity of ZnO/CuO nanocomposite for the degradation of textile dye on visible light illumination. *Mater Sci Eng C*. 2013;33(1):91–98. doi:10.1016/j.msec.2012.08.011
4. Anicai L, Petica A, Patroi D, Marinescu V, Prioteasa P, Costovici S. Electrochemical synthesis of nanosized TiO2 nanopowder involving choline chloride based ionic liquids. *Mater Sci Eng*. 2015;199:87–95. doi:10.1016/j.mseb.2015.05.005
5. Qiufen H, Yang T, Zhang X, Tang A, Ouyang J. Solid-state synthesis and electrochemical property of SnO2/NiO nanomaterials. *J Alloys Compd*. 2008;459(1–2):98–102. doi:10.1016/j.jallcom.2007.04.258
6. Fang J, Ma J, Sun Y, Z.Liu CG, Gao C. Electrochemical synthesis of nanocrystalline SrNb2O6 powders and characterization of their photocatalytic property. *Mater Sci Eng, B*. 2011;176(9):701–705. doi:10.1016/j.mseb.2011.02.021
7. Das S, Srivastava VC. An overview of the synthesis of CuO-ZnO nanocomposite for environmental and other applications. *Nanotechnol Rev*. 2018;7(3):267–282. doi:10.1515/ntrev-2017-0144
8. Alnahari H, Al-Sharab A, Al-Hammadi AH, Al-Odayni A. Synthesis of glycine-mediated CuO–Fe2O3–MgO nanocomposites: structural, optical, and antibacterial properties. *Compos Adv Mater*. 2023;32:26349833231176838. doi:10.1177/26349833231176838
9. Balamurugan S, Balu AR, Narasimman V, et al. Multi metal oxide CdO–Al2O3–NiO nanocomposite—synthesis, photocatalytic and magnetic properties. *Mater Res Express*. 2018;6(1):015022. doi:10.1088/2053-1591/aae5af

10. Sharma RK, Kumar D, Ghose R. Synthesis of nanocrystalline ZnO–NiO mixed metal oxide powder by homogeneous precipitation method. *Ceram Int*. 2016;42(3):4090–4098. doi:10.1016/j.ceramint.2015.11.081
11. Yang W, Deng X, Huang W, Qing X, Shao Z. The physicochemical properties of graphene nanocomposites influence the anticancer effect. *J Oncol*. 2019;2019:1–10. doi:10.1155/2019/7254534
12. Jaya Seema DM, Saifullah B, Selvanayagam M, et al. Designing of the anticancer nanocomposite with sustained release properties by using graphene oxide nanocarrier with phenethyl isothiocyanate as anticancer agent. *Pharmaceutics*. 2018;10(3):109. doi:10.3390/pharmaceutics10030109
13. Kaplan A. The nanocomposites designs of phytomolecules from medicinal and aromatic plants: promising anticancer-antiviral applications. Beni-Suef Univ. *J Basic Appl Sci*. 2022;11(1):17. doi:10.1186/s43088-022-00198-z
14. Ahamed M, Akhtar MJ, Khan MA, Alhadlaq HA. Enhanced anticancer performance of eco-friendly-prepared Mo-ZnO/RGO nanocomposites: role of oxidative stress and apoptosis. *ACS omega*. 2022;7(8):7103–7115. doi:10.1021/acsomega.1c06789
15. Nazir S, Khan MU, Al-Arjan WS, Razak SI, Javed A, Kadir MR. Nanocomposite hydrogels for melanoma skin cancer care and treatment: in-vitro drug delivery, drug release kinetics and anti-cancer activities. *Arab J Chem*. 2021;14(5):103120. doi:10.1016/j.arabjc.2021.103120
16. Ghasempour A, Dehghan H, Ataee M, et al. Cadmium sulfide nanoparticles: preparation, characterization, and biomedical applications. *Molecules*. 2023;28(9):3857. doi:10.3390/molecules28093857
17. Zahera M, Khan SA, Khan IA, et al. Cadmium oxide nanoparticles: an attractive candidate for novel therapeutic approaches. *Colloids Surf A*. 2020;585:124017. doi:10.1016/j.colsurfa.2019.124017
18. Juan CA, Lastra JMP, Plou FJ, Lebena EP. The chemistry of reactive oxygen species (ROS) revisited: outlining their role in biological macromolecules (DNA, lipids and proteins) and induced pathologies. *Int J Mol Sci*. 2021;22(9):4642. doi:10.3390/ijms22094642
19. Abyar S, Khandar AA, Salehi R, et al. In vitro nephrotoxicity and anticancer potency of newly synthesized cadmium complexes. *Sci Rep*. 2019;9(1):14686. doi:10.1038/s41598-019-51109-92
20. Mazhar A, Elkholy NS, Yousif NM, Shalaby MS. Investigations of structural, optical, thermal, and spectroscopic characteristics of CdO-Ni nanoparticles employed in anti-cancer activities for cancer cells. *Results Chem*. 2023;6:101204. doi:10.1016/j.rechem.2023.101204
21. Makkawi AJJ, Aysa NH, Gassim F-AG. Anticancer activity of zinc oxide and zinc oxide/cadmium sulfide nanocomposites. *Asian J Pharm Clin Res*. 2019;535–539. doi:10.22159/ajpcr.2019.v12i2.26265
22. Shalaby M, Kodous AS, Yousif N. Structural, optical characteristics and anti-cancer effect of Cd0. 99Ni0. 01O nanoparticles on human neuroblastoma and cervical cancer cell lines. *Inorg Chem Commun*. 2022;141:109583. doi:10.1016/j.inoche.2022.109583
23. Kladko DV, Falchevskaya AS, Serov NS, Prilepskii AY. Antibacterial activity of solvothermal obtained ZnO nanoparticles with different morphology and photocatalytic activity against a dye mixture: methylene blue, rhodamine B and methyl Orange. *Int J Mol Sci*. 2023;24(6):5677. doi:10.3390/ijms22105266
24. Motelica L, O.Oprea BV, Ficai A, Ficai D, Andronescu E, Holban AM. Influence of the alcohols on the zno synthesis and its properties: the photocatalytic and antimicrobial activities. *Pharmaceutics*. 2022;14(12):2842. doi:10.3390/ijms24065677
25. Motelica L, B.Vasile AF, Surdu A, et al. Nanomaterial shape influence on cell behavior. *Int J Mol Sci*. 2021;22(10):5266. doi:10.3390/pharmaceutics14122842
26. Jin S-E, Jin H-E. Multiscale metal oxide particles to enhance photocatalytic antimicrobial activity against Escherichia coli and M13 bacteriophage under dual ultraviolet irradiation. *Pharmaceutics*. 2021;13(2):222. doi:10.3390/pharmaceutics13020222
27. Abudayyak M, Guzel E, Özhan G. Cupric oxide nanoparticles induce cellular toxicity in liver and intestine cell lines. *Adv Pharm Bull*. 2020;10(2):213. doi:10.34172/apb.2020.025
28. Kalaiarasi A, Sankar R, Anusha C, et al. Copper oxide nanoparticles induce anticancer activity in A549 lung cancer cells by inhibition of histone deacetylase. *Biotechnol Lett*. 2018;40:249–256. doi:10.1007/s10529-017-2463-6
29. Kang T, Guan R, Chen X, Song Y, Jiang H, Zhao J. In vitro toxicity of different-sized ZnO nanoparticles in Caco-2 cells. *Nanoscale Res Lett*. 2013;8:1–8.
30. Selvakumari SD, R.Deepa VM, P. Subhashini NL. Anti cancer activity of ZnO nanoparticles on MCF7 (breast cancer cell) and A549 (lung cancer cell). *ARPN J Eng Appl Sci*. 2015;10(12):5418–5421.
31. Jana TK, Jana SK, Kumar A, et al. The antibacterial and anticancer properties of zinc oxide coated iron oxide nanotextured composites. *Colloids Surf B*. 2019;177:512–519. doi:10.1016/j.colsurfb.2019.02.041
32. Mohamed HH, Youssef TE, Fadeel DA. Magnetic ZnO/CdO nanocomposite for effective drug delivery system for cancer therapy. *Biointerf Res Appl Chem*. 2022;2022:1. doi:10.33263/BRIAC131.060
33. Kannan K, Sivasubramanian D, Seetharaman P, Sivaperumal S. Structural and biological properties with enhanced photocatalytic behaviour of CdO-MgO nanocomposite by microwave-assisted method. *Optik*. 2020;204:164221. doi:10.1016/j.ijleo.2020.164221
34. Elemike EE, Onwudiwe DC, Singh M. Eco-friendly synthesis of copper oxide, zinc oxide and copper oxide–zinc oxide nanocomposites, and their anticancer applications. *J Inorg Organomet Polym Mater*. 2020;30(2):400–409. doi:10.1007/s10904-019-01198-w
35. Lefojane LR, B.T.Sone NM, P.Mfengwana SM, Maaza M, Sekoacha MP. CdO/CdCO3 nanocomposite physical properties and cytotoxicity against selected breast cancer cell lines. *Sci Rep*. 2021;11(1):30. doi:10.1038/s41598-020-78720-5
36. Skheel AZ, Jaduaa MH, Abd AN. Green synthesis of cadmium oxide nanoparticles for biomedical applications (antibacterial, and anticancer activities). *Mater Today Proc*. 2021;45:5793–5799. doi:10.1016/j.matpr.2021.03.168
37. Rehman WU, Khattak MT, Saeed A, et al. Co3O4/NiO nanocomposite as a thermocatalytic and photocatalytic material for the degradation of malachite green dye. *J Mater Sci Mater Electron*. 2023;34(1):15. doi:10.1007/s10854-022-09428-7
38. Karthik K, Dhanuskodi S, Gobinath C, Sivaramakrishnan S. Microwave-assisted synthesis of CdO–ZnO nanocomposite and its antibacterial activity against human pathogens. *Spectrochim Acta Part A Mol Biomol Spectrosc*. 2015;139:7–12. doi:10.1016/j.saa.2014.11.079
39. Munusamy TD, Yee CS, Khan MMR. Construction of hybrid g-C3N4/CdO nanocomposite with improved photodegradation activity of RhB dye under visible light irradiation. *Adv Powder Technol*. 2020;31(7):2921–2931. doi:10.1016/j.apt.2020.05.017
40. Rahman MM, Hussain MM, Asiri AM. Ultrasensitive and label-free detection of creatine based on CdO nanoparticles: a real sample approach. *New J Chem*. 2017;41(14):6667–6677. doi:10.1039/C6NJ04101A
41. Krishna KG, Parne SR, Nagaraju P. ZnO/CdO island-like porous nanocomposite as an ultra-sensitive sensor for BTX detection at room temperature. *Surf Interfaces*. 2024;44:103631. doi:10.1016/j.surfin.2023.103631

42. Al-Sharabi A, Sada'a KS, R.A.Shukor AAL-O, Abd-Shukor R. Structure, optical properties and antimicrobial activities of MgO–Bi2− x Cr x O3 nanocomposites prepared via solvent-deficient method. *Sci Rep*. 2022;12(1):10647. doi:10.1038/s41598-022-14811-9
43. Elayarajaa M, Punithavathya IK, Jeyakumara SJ, Praveenb P. Experimental investigation of the inhibitory behavior of cdo nanoparticleson co-precipitation method.
44. Raba-Páez AM, Malafatti JD, Parra-Vargas CA, Paris EC, Rincón-Joya M. Effect of tungsten doping on the structural, morphological and bactericidal properties of nanostructured CuO. *PLoS One*. 2020;15(9):e0239868. doi:10.1371/journal.pone.0239868
45. Abdulwahab A, Al-Mahdi EA, Al-Osta A, Qaid AA. Structural, optical and electrical properties of CuSCN nano-powders doped with Li for optoelectronic applications. *Chin J Phys*. 2021;73:479–492. doi:10.1016/j.cjph.2021.06.026
46. Munawar T, Iqbal F, Yasmeen S, Mahmood K, Hussain A. Multi metal oxide NiO-CdO-ZnO nanocomposite–synthesis, structural, optical, electrical properties and enhanced sunlight driven photocatalytic activity. *Ceram Int*. 2020;46(2):2421–2437. doi:10.1016/j.ceramint.2019.09.236
47. Ma J, Wang K, Li L, Zhang T, Kong Y, Komarneni S. Visible-light photocatalytic decolorization of Orange II on Cu2O/ZnO nanocomposites. *Ceram Int*. 2015;41(2):2050–2056. doi:10.1016/j.ceramint.2014.09.137
48. Aziz SN, Abdulwahab A, Aldeen TS. Synthesis and characterization of (CdO-CuOCo3O4) mixed metal oxides nanocomposite. *Sana'a Univ J Appl Sci Technol*. 2024;2(2):116–123. doi:10.59628/jast.v2i2.874
49. Rastar A, Yazdanshenas ME, Rashidi A, Bidoki SM. Theoretical review of optical properties of nanoparticles. *J Eng Fiber Fabr*. 2013;8 (2):155892501300800211. doi:10.1177/155892501300800211
50. Ahmed AAA, Abdulwahab AM, Talib ZA, Salah D, Flaifel MH. Magnetic and optical properties of synthesized ZnO–ZnFe2O4 nanocomposites via calcined Zn–Fe layered double hydroxide. *Opt Mater*. 2020;108:110179. doi:10.1016/j.optmat.2020.110179
51. Aldeen TS, Mohamed HEA, Maaza M. Bio-inspired Single Phase Monteponite cdo nanoparticles via natural extract of Phoenix roebelenii palm leaves. *J Inorg Organomet Polym Mater*. 2020;30:4691–4701. doi:10.1007/s10904-020-01600-y
52. Khammarnia S, Saffari J, Ekrami-Kakhki M-S. Synthesis of La2MnFe2O7 and La2CuFe2O7 magnetic nanocomposites (nano mixed metal oxides) as efficient photocatalyst for organic dye removal. *Chem Rev Lett*. 2024;7(1):123–133.
53. Akyüz D. rGO-TiO2-CdO-ZnO-Ag photocatalyst for enhancing photocatalytic degradation of methylene blue. *Opt Mater*. 2021;116:111090. doi:10.1016/j.optmat.2021.111090
54. Li D, Song H, Meng X, et al. Effects of particle size on the structure and photocatalytic performance by alkali-treated TiO2. *Nanomaterials*. 2020;10(3):546. doi:10.3390/nano10030546
55. Ishfaq M, Hassan W, Sabir M, et al. Wet-chemical synthesis of ZnO/CdO/CeO2 heterostructure: a novel material for environmental remediation application. *Ceram Int*. 2022;48(23):34590–34601. doi:10.1016/j.ceramint.2022.08.046
56. Alam MW, Al Qahtani HS, Souayeh B, et al. Novel copper-zinc-manganese ternary metal oxide nanocomposite as heterogeneous catalyst for glucose sensor and antibacterial activity. *Antioxidants*. 2022;11(6):1064. doi:10.3390/antiox11061064
57. Freitas C, Müller RH. Effect of light and temperature on zeta potential and physical stability in solid lipid nanoparticle (SLN™) dispersions. *Int J Pharm*. 1998;168(2):221–229. doi:10.1016/S0378-5173(98)00092-1
58. Aziz SN, Abdulwahab AM, Aldeen TS, Alqabili DMA. Synthesis, characterization, and evaluation of antibacterial and antifungal activities of CuO-ZnO-Co3O4 nanocomposites. *Heliyon*. 2024;10(18):e37802. doi:10.1016/j.heliyon.2024.e37802
59. Hussein ON, AL-Jawad SM, Imran NJ. Efficient antibacterial activity enhancement in Fe/Mn co-doped CuS nanoflowers and nanosponges. *Bull Mater Sci*. 2023;46(3):139. doi:10.1007/s12034-023-02964-w
60. Yang H, Liu C, Yang D, Zhang H, Xi Z. Comparative study of cytotoxicity, oxidative stress and genotoxicity induced by four typical nanomaterials: the role of particle size, shape and composition. *J Appl Toxicol*. 2009;29(1):69–78. doi:10.1002/jat.1385
61. De Berardis B, Civitelli G, Condello M, et al. Exposure to ZnO nanoparticles induces oxidative stress and cytotoxicity in human colon carcinoma cells. *Toxicol Appl Pharmacol*. 2010;246(3):116–127. doi:10.1016/j.taap.2010.04.012
62. Singh N, Manshian B, Jenkins GJS, et al. NanoGenotoxicology: the DNA damaging potential of engineered nanomaterials. *Biomaterials*. 2009;30 (23–24):3891–3914. doi:10.1016/j.biomaterials.2009.04.009
63. Abedini A, Rostami M, Banafshe HR, Rahimi-Nasrabadi M, A.Sobhani-Nasab MRG, Ganjali MR. Utility of biogenic iron and its bimetallic nanocomposites for biomedical applications: a review. *Front Chem*. 2022;10:893793. doi:10.3389/fchem.2022.893793
64. Sabouri Z, Sabouri M, Moghaddas SS, Mostafapour A, Samarghandian S, Darroudi M. Plant-mediated synthesis of Ag and Se dual-doped ZnO-CaO-CuO nanocomposite using Nymphaea alba L. extract: assessment of their photocatalytic and biological properties. *Biomass Convers Biorefin*. 2023;1–11. doi:10.1007/s13399-023-04984-2
65. Smitha S, Krishna PA, Tharayil NJ. Cytotoxic and anticancer activity of mixed metal oxide FeO: mnO nanostructures. *Mater Today Proc*. 2022;66:2245–2250. doi:10.1016/j.matpr.2022.06.096
66. Elsayed KA, Alomari M, Drmosh QA, et al. Fabrication of ZnO-Ag bimetallic nanoparticles by laser ablation for anticancer activity. *Alex Eng J*. 2022;61(2):1449–1457. doi:10.1016/j.aej.2021.06.051
67. Arakha M, Roy J, Nayak PS, Mallick B, Jha S. Zinc oxide nanoparticle energy band gap reduction triggers the oxidative stress resulting into autophagy-mediated apoptotic cell death. *Free Radic Biol Med*. 2017;110:42–53. doi:10.1016/j.freeradbiomed.2017.05.015
68. Mejia-Mendez JL, Reza EE, Sanchez A, et al. Exploring the cytotoxic and antioxidant properties of lanthanide-doped ZnO nanoparticles: a study with machine learning interpretation. *J Nanobiotechnol*. 2024;22(1):687. doi:10.1186/s12951-024-02957-9
69. Ahamed M, Khan MAM, Akhtar MJ, Alhadlaq HA, Alshamsan A. Ag-doping regulates the cytotoxicity of TiO2 nanoparticles via oxidative stress in human cancer cells. *Sci Rep*. 2017;7(1):17662. doi:10.1038/s41598-017-17559-9
70. Abbas F, Iqbal J, Maqbool Q, et al. ROS mediated malignancy cure performance of morphological, optical, and electrically tuned Sn doped CeO2 nanostructures. *AIP Adv* 2017;7(9). doi:10.1063/1.4990790
71. Bhavana S, Kusuma CG, Gubbiveeranna V, Sumachirayu CK, Ravikumar H, Nagaraju S. Green route synthesis of copper oxide nanoparticles using Vitex altissima [L] leaves extract and their potential anticancer activity against A549 cell lines and its apoptosis induction. *Inorg Nano-Met Chem*. 2024;54(10):1012–1025. doi:10.1080/24701556.2022.2081195
72. Abdollahzadeh H, Pazhang Y, Zamani A, Sharafi Y. Green synthesis of copper oxide nanoparticles using walnut shell and their size dependent anticancer effects on breast and colorectal cancer cell lines. *Sci Rep*. 2024;14(1):20323. doi:10.1038/s41598-024-71234-4
73. Rahman CS, Mustafa TA. Cytotoxic effect of zinc oxide nanoparticle and diode laser combination in colorectal cancer in vitro via induction of cell cycle arrest and apoptosis. *JABET* 2023;6(2):527. doi:10.5455/jabet.2023.d146

74. Berehu HM, Patnaik S. Biogenic Zinc Oxide Nanoparticles synthesized from Tinospora Cordifolia induce oxidative stress, mitochondrial damage and apoptosis in Colorectal Cancer. *Nanotheranostics*. 2024;8(3):312. doi:10.7150/ntno.84995
75. Al Sharie AH, El-Elimat T, Darweesh RS, et al. Green synthesis of zinc oxide nanoflowers using Hypericum triquetrifolium extract: characterization, antibacterial activity and cytotoxicity against lung cancer A549 cells. *Organomet Chem*. 2020;34(8):e5667. doi:10.1002/aoc.5667
76. Jafarirad S, Taghizadeh PM, Divband B. Biosynthesis, characterization and structural properties of a novel kind of Ag/ZnO nanocomposites in order to increase its biocompatibility across human A549 cell line. *BioNanoScience*. 2020;10:42–53. doi:10.1007/s12668-019-00685-1
77. Abhilash PK, Jegajeevanram P, Prabu P, et al. Multifunctional cerium oxide-copper oxide nanocomposites prepared via one-pot engineering precipitation: antimicrobial, antioxidant and anticancer activities. *J Indian Chem Soc*. 2025;102(1):101525. doi:10.1016/j.jics.2024.101525
78. Selim S, Almuhayawi MS, Alruhaili MH, et al. Synthesis, characterization, anticancer, antibacterial and antifungal activities of nanocomposite based on tertiary metal oxide Fe2O3@ CuO@ ZnONPs, starch, ethylcellulose and collagen. *Int J Biol Macromol*. 2025;140376. doi:10.1016/j.ijbiomac.2025.140376
79. Abdulwahab AM, Al-Adhreai AA, AlHammadi AH, et al. Synthesis, characterization, and anti-cancer activity evaluation of Ba-doped CuS nanostructures synthesized by the co-precipitation method. *RSC Adv*. 2025;15(6):4669–4680. doi:10.1039/D4RA07078J